Realizing a negative index metamaterial by controlling hybridization of trapped modes

Redha Abdeddaim, Abdelwaheb Ourir,* and Julien de Rosny
Institut Langevin, UMR 7587, ESPCI ParisTech, CNRS, Laboratoire Ondes et Acoustique (LOA), 10 rue Vauquelin, F-75231 Paris, Cedex 05, France
(Received 16 June 2010; published 3 January 2011)

We report a way to realize a left-handed metamaterial based on hybridization of trapped modes. This results from the stacking of two identical structures. The introduction of a structural asymmetry tunes the trapped modes without modifying Coulomb interactions. The negative index band is obtained thanks to the overlapping of two hybrid modes coming from two different modes. This approach is validated numerically and experimentally.

DOI: 10.1103/PhysRevB.83.033101 PACS number(s): 41.20.Jb, 42.25.Ja, 73.20.Mf, 81.05.Zx

A left-handed material[1] (LHM) is a composite material characterized by simultaneous negative values of the real parts of electrical permittivity (ε) and magnetic permeability (μ). The most common and well-known approach to realize a LHM is the combination of two distinct meta-atoms with respectively negative ε and negative μ, like the association of continuous wires[2] and split-ring resonators[3,4] (SRRs). Other structures have been proposed to give a negative index such as a structure with only one meta-atom where the electrical and magnetic resonances overlap as for S-shaped structures.[5] All these configurations require the application of a magnetic field perpendicular to the resonator plane. Consequently, a large number of planes has to be stacked laterally, which is difficult to realize in the optical domain. A more compact design is fishnet. It behaves like a combination of pairs of short slabs, which provides negative permeability and continuous wires where plasmonic-like modes induce negative permittivity.[6] However, all the unit cells must be physically interconnected in the direction of the electrical field. The large fraction of metal contained in this structure induces high-level losses in the optical regime.[7] Recently, a novel way to generate a negative index was demonstrated.[8–11] It consists of the inversion of the hybridization of two plasmon modes. The hybridization results from the stacking of two identical atoms. These two atoms are twisted or shifted in regards to one another. In this way, a geometrical asymmetry is introduced, that is, an asymmetry in the direction of propagation. The first observation of this phenomenon occurred in the case of the coupling of cut wires. Indeed, a wire-wire coupling results in the formation of two energetically separated plasmonic modes.[12] The lower and higher frequency modes exhibit negative μ and negative ε respectively. This phenomenon has been also observed in the case of stacked SRRs.[13] With this novel coupling configuration, it has become possible to realize a thin metafilm that exhibits a negative index.[11,13,14] Breaking the geometrical symmetry between the two stacked meta-atoms leads to the inversion of the hybridization modes. The negative index is present when the two modes coming from hybridization resonate around the same frequency. This hybridization inversion by a geometrical asymmetry is due to the modification of the Coulomb interactions between the two stacked meta-atoms. Metamaterials obtained in such ways are called stereometamaterials in reference to the stereochemistry of materials with the same chemical formula but different spatial arrangements of atoms.[14]

In the present work, we propose a new kind of stereometamaterial composed of the same meta-atoms with the same spatial arrangements. Here, we do not break the symmetry between the two stacked structures (geometrical asymmetry) but the symmetry of the structure itself (structural asymmetry). In this way, we obtain trapped modes, also called dark modes.[15,16] The coupling of two identical asymmetric structures yields the hybridization of these trapped modes. The aim is to overlap two resonant hybrid modes with negative μ and negative ε, respectively. Here, it is achieved with two hybrid modes stemming from the hybridization of two different modes. We show that a negative index is achieved with this method. The proposed metamaterial consists of a periodic arrangement of identical meta-atoms. They are arranged on a square lattice with a 44-mm period. The meta-atom is a four-gap resonator (FG) [see Fig. 1(a)]. They are printed on a 3.5-mm-thick FR4 dielectric substrate. The FG structure is either symmetric (SFG) when the four gap sizes are equal or asymmetric (AFG) when one gap is different from the others. In this Brief Report, only the size, g_a, of the gap at the bottom of the cell [see Fig. 1(a)] is variable. All the other gaps have a fixed size set to $g = 1.2$ mm.

We study this structure in two different polarizations. In the first polarization (E_H), the electrical field is perpendicular to the symmetry axis of the AFG; that is, the electrical field is parallel to the arm that contains the gap g_a. In the second polarization (E_V), the electrical field is parallel to the symmetry axis; that is, the electrical field is perpendicular to the arm of the gap g_a [see Fig. 1(a)].

Figure 2(a) presents several transmission spectra obtained by simulation of SFG and AFG for the vertical and the horizontal polarization. Because of the perfect symmetry of the SFG, its response is the same for both polarizations and is characterized by a fundamental resonance frequency (ω_0). When the size ($g_a = 9$ mm) of the bottom gap is modified, the symmetry of the structure is broken, and both polarizations show two resonant modes instead of one. For the vertical polarization, the resonant frequencies ω_{0V},ω_{1V} are larger than ω_0, while for the horizontal one, ω_{0H},ω_{1H} are located around ω_0.

To understand the nature of the resonant modes and their dependence on gap dimensions and on polarization, we plot in Fig. 2(b) the electrical energy density map and the current directions on each arm. We also propose an atomic-like representation of the resonance frequencies with a schematic view

 ©2011 The American Physical Society

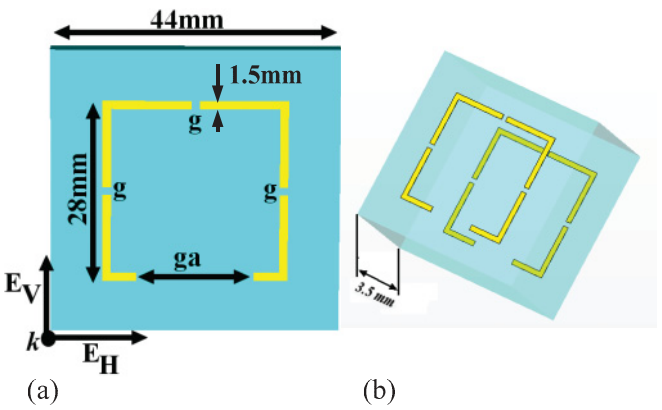

FIG. 1. (Color online) (a) Unit cell of AFG. The four-gap square pattern is etched on dielectric substrate (FR4). The thickness of the copper layer equals 1/10 mm. (b) Elementary cell of two stacked AFGs.

of the eigenstates. These depend on the current orientation on each arm. In the case of SFG, the horizontal and vertical symmetries of the unit cell imply that at low frequencies the four modes are either symmetric or antisymmetric with respect to the symmetry axes. Consequently, a horizontally polarized wave can only couple with the mode that is symmetric and antisymmetric with respect to the horizontal and the vertical axes, respectively. The roles of the vertical and horizontal axes are swapped for a vertically polarized incident wave. These two last modes ⊞ and ⊞ of Fig. 2(b)] are degenerated with the same resonant frequency ω_0. It is enlightening to analyze AFG in terms of the weak coupling of the SFG modes. Because the vertical of AFG axis is still a symmetric axis, the mode coupling can only occur between modes that are either symmetric or antisymmetric with respect to this axis. The coupling of the symmetric modes gives rise to two modes with modified current intensity distribution [see "horizontal polarization" on Fig. 2(b)]. The fundamental mode at frequency ω_0 is blue shifted to ω_{1H}. Indeed, the modes at ω_0 (SFG) and ω_{1H} (AFG) are basically the same. As for the mode ⊞, it weakly interacts with the fundamental mode ⊞. Because of the modification of the current distribution, the perturbed mode can now be excited by a horizontally polarized wave. This explanation is confirmed by the current distribution at resonance frequency ω_{0H}. Because of the weak coupling, this mode is a trapped one. Likewise, in the E_V polarization, the mode ω_{0V} is in the fundamental one and the mode ω_{1V} is in the trapped one.

By controlling the gap size, we modify the intervals between the resonant frequencies. However, it is a very difficult task, if not impossible, to obtain the analytical expressions of these frequencies. That is why we choose to estimate their dependence on g_a with a second-order polynomial fit on the simulation results. The polynomial expression is defined by

$$\omega_{ip} = \alpha_{ip} g_a^2 + \beta_{ip} g_a + \gamma_{ip}. \quad (1)$$

The polarization is identified by $p = H$ or $p = V$. Subscript i, which can be equal to 0 or 1, represents the index of the resonance. The coefficients α, β, and γ deduced from the polynomial fit are shown in Table I.

TABLE I. Polynomial coefficients α, β, and γ of Eq. (1) at resonant frequencies ω_{0H}, ω_{1H}, ω_{0V}, and ω_{1V}.

	ω_{0H}	ω_{1H}	ω_{0V}	ω_{1V}
α	−0.0005	−0.0012	−0.00008	−0.0008
β	0.0255	0.0644	0.017	0.0297
γ	2.5562	3.452	3.4612	4.1416

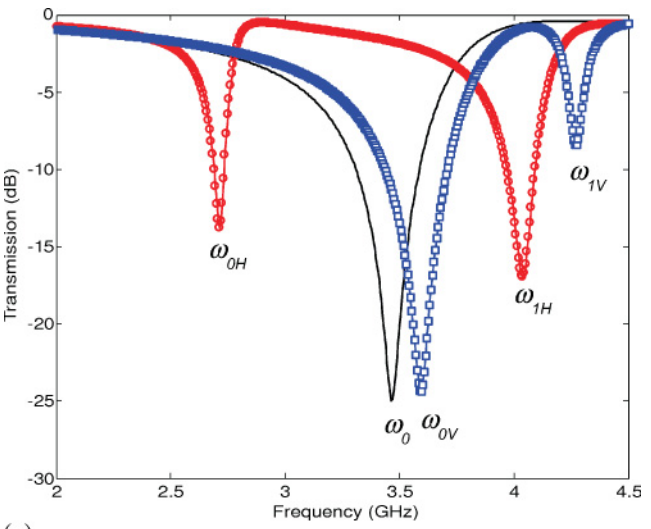

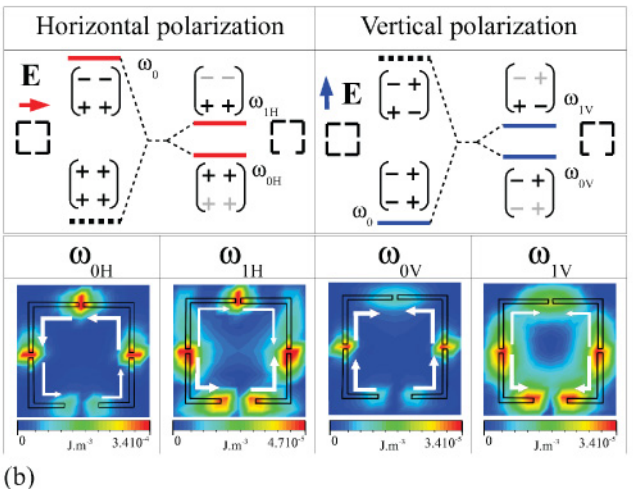

FIG. 2. (Color online) (a) Normal incidence transmission trough: SFG with $g = g_a = 1.2$ mm (−) and AFG with g_a now equal to 9 mm, horizontal polarization (□), vertical polarization (○). (b) Atomic-like representation of the weak coupling between modes when the cell symmetry is broken for the two polarizations. The corresponding eigenstate is represented just above or below the level. It shows the orientation (clockwise [+] or counterclockwise [−]) of the current on each square edge. A light gray + or − means that the current intensity is smaller as a result of the coupling. The black dashed line levels cannot be externally excited by a vertically or horizontally polarized wave. On the bottom, the energy density maps of the electric field at the four resonances. Arrows on the energy density map show the directions of the current intensity, and the thickness of the arrows give an idea of the current intensity.

Table I confirms that the modes are differently affected by the modification of the gap size. Indeed, in contrast to the normal modes, the trapped ones interact strongly with the gap size.

Now, we stack a second AFG on the opposite side of the substrate [see Fig. 1(b)]. The thickness of the FR4 substrate (3.5 mm) is chosen to ensure a sufficiently strong hybridization. Consequently, the stacking of two AFG induces the splitting of each mode ω_{ip} into two modes: one antisymmetric (ω_{ip-}) and one symmetric (ω_{ip+}) with respect to the stack plane.[14] The four symmetric (antisymmetric) modes radiate like electric (magnetic) dipoles and therefore can exhibit a resonant negative permittivity (permeability).

The coupling between the two AFGs is similar to the coupling between two resonators composed of an inductor L and a capacitor C. The Lagrangian of two coupled LC resonators is given by[17]

$$\mathcal{L} = (L/2)\left(\dot{Q}_1^2 - \omega_0^2 Q_1^2\right) + (L/2)\left(\dot{Q}_2^2 - \omega_0^2 Q_2^2\right) + M\dot{Q}_1^2\dot{Q}_2^2, \quad (2)$$

where Q_1 and Q_2 are oscillatory charges and M is the mutual inductance. By minimizing the action associated to this Lagragian, the two resonance frequencies of the hybridized modes are

$$w_\pm = w_0\sqrt{1 \pm k}, \quad (3)$$

where $\kappa = M/L$. This coefficient depends not only on the thickness of the substrate but also on the resonant frequency ω_0.[11] Within our working frequency band, the variation of κ is fit well by a third-order polynomial expansion:

$$k(w_0) \approx -0.011w_0^3 + 0.1228w_0^2 - 0.4688w_0 + 0.7885. \quad (4)$$

By combining (1), (3), and (4), eight polynomial expressions for the hybrid modes as a function of the asymmetric gap size g_a are deduced.

Now, to obtain a negative index, the aim is to find two hybrid modes, one symmetric and one antisymmetric, characterized by the same resonant frequency. However, in the horizontal polarization, this condition cannot be fulfilled. Effectively, the frequency resonance of the two original modes (before stacking) are too far one from the other one. As a result, the hybrid modes are also too far away to allow frequency crossing. Hence, the magnetic hybrid mode cannot overlap with the electric hybrid mode in such polarization. In vertical polarization, the variations of the angular frequencies ω_{0V-}, ω_{0V+}, ω_{1V-}, and ω_{1V+} of the four hybridization modes are plotted in Fig. 3(a). The gap perturbation cannot invert the hybridization of the same mode. However, the second magnetic mode frequency (ω_{1V-}) is sufficiently close to and increases sufficiently faster than the first electrical mode frequency (ω_{0V+}) to finally cross it. The fast increase of ω_{1V-} is because a trapped mode is much more sensitive to geometric modification. At the crossing (here $g_a = 12$ mm and $\omega/2\pi \approx 3.9$ GHz), both ϵ and μ are negative, and a negative index can be obtained. Figure 3(b) shows the energy level representation of these two modes, the normal one and the trapped one, before and after hybridization. These diagrams reveal the mechanism of the hybridization and how the inversion is obtained as a function of the gap size.

We experimentally realize such a metamaterial. The measurements are performed in an anechoic chamber with a vectorial network analyzer and horn antennas. We measure the transmission and reflection parameters of a periodic arrangement of asymmetric stacked cells ($g_a = 12$ mm) in

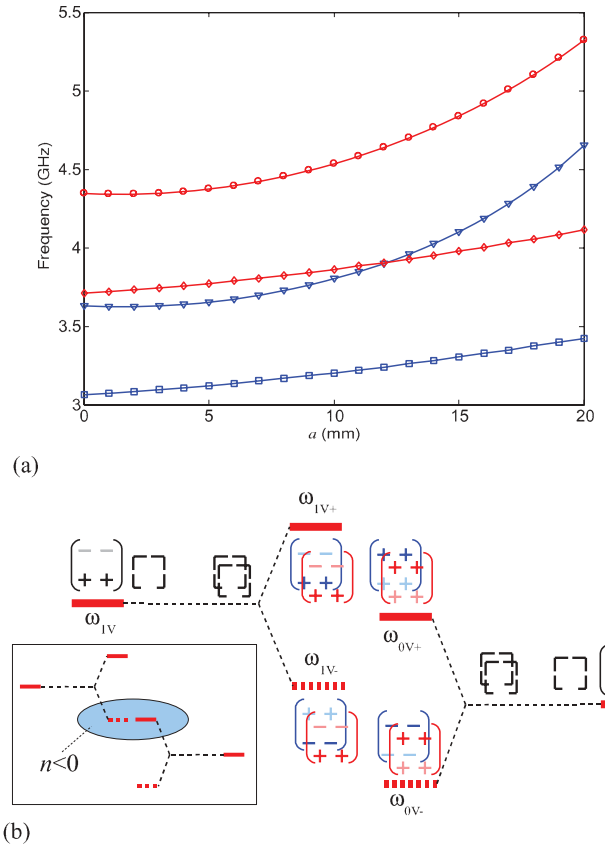

FIG. 3. (Color online) (a) Evolution of the four hybrid mode resonances with respect to the gap size a. The lines with marks □, ▽, ◇, and ○ correspond to ω_{0V-}, ω_{0V+}, ω_{1V-}, and ω_{1V+}, respectively. (b) Atomic energy level representation of the hybridization of the modes involved in the negative index. The corresponding eigenstate is represented just above or below the level. It shows the sign of the current direction [see Fig. 2(b)] on each square edge and on each side of the substrate. The inset shows the frequency crossing with the negative refraction index when $g_a = 12$ mm.

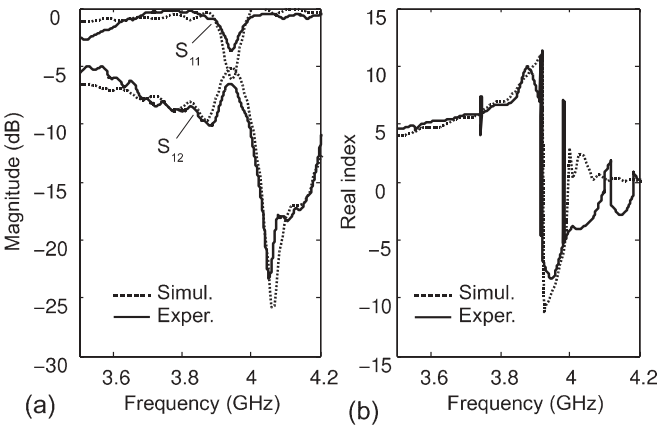

FIG. 4. (a) Experimental (simulated) transmission (S_{11}) and reflection (S_{12}) parameters are plotted in continuous (dashed) line of a vertically polarized wave. (b) Real part of the refraction indexes recovered from the experimental and simulation S parameters.

vertical polarization. The total lattice size is 270 mm by 270 mm. Figure 4(a) shows the transmission coefficients. There is excellent agreement between the experimental and simulation results. Hence, measurements confirm the theoretical approach. A transmission band located around 4 GHz as a result of the overlap of electric and magnetic hybridized modes is clearly observed. The real parts of the refraction index are plotted in Fig. 4(b). The index becomes negative where the transmission band appears. The negative sign of the index demonstrates that it is possible to obtain an effect equivalent to inverted hybridization, but here it is obtained with symmetric and antisymmetric hybrid modes that originate in different modes thanks to parametric control of the hybridization.

In conclusion, by controlling the gap size, we have shown that trapped modes can be easily excited and tuned. By stacking two identical cells, we have demonstrated numerically and experimentally that a left-handed stereometamaterial can be obtained by the hybridization process. In contrast to previous works, this is achieved by breaking the symmetry of the cell and not the symmetry between the two stacked cells. With modern lithography techniques, this cell pattern can be made at the nanoscale to build optical metamaterials with negative index. The advantage of this new design is to reduce drastically (up to a factor of 2) the dimension cell compared to stereometamaterial based on geometrical translation asymmetry.

*a.ourir@espci.fr, [http://www.institut-langevin.espci.fr/].

[1] V. G. Veselago, Sov. Phys. Usp. **10**, 509 (1968).
[2] J. B. Pendry, A. J. Holden, D. J. Robbins, and W. J. Stewart, J. Phys. Condens. Matter **10**, 4785 (1998).
[3] J. B. Pendry, A. J. Holden, D. J. Robbins, and W. J. Stewart, IEEE T. Microw. Theory **47**, 2075 (1999).
[4] D. R. Smith, W. J. Padilla, D. C. Vier, S. C. Nemat-Nasser, and S. Schultz, Phys. Rev. Lett. **84**, 4184 (2000).
[5] H. Chen, L. Ran, J. Huangfu, X. Zhang, K. Chen, T. M. Grzegorczyk, and J. A. Kong, Phys. Rev. E **70**, 057605 (2004).
[6] M. Kafesaki, I. Tsiapa, N. Katsarakis, T. Koschny, C. M. Soukoulis, and E. N. Economou, Phys. Rev. B **75**, 235114 (2007).
[7] B. Kanté, S. N. Burokur, A. Sellier, A. de Lustrac, and J. M. Lourtioz, Phys. Rev. B **79**, 075121 (2009).
[8] V. A. Podolskiy, A. K. Sarychev, and V. M. Shalaev, J. Nonlinear Opt. Phys. Mater. **11**, 65 (2002).
[9] G. Dolling, C. Enkrich, M. Wegener, J. Zhou, and C. Soukoulis, Opt. Lett. **30**, 3198 (2005).
[10] S. Zhang, W. J. Fan, N. C. Panoiu, K. J. Malloy, R. M. Osgood, and S. R. J. Brueck, Phys. Rev. Lett. **95**, 137404 (2005).
[11] S. Linden, M. Decker, and M. Wegener, Phys. Rev. Lett. **97**, 083902 (2006).
[12] A. Christ, O. J. F. Martin, Y. Ekinci, N. A. Gippius, and S. G. Tikhodeev, Nano Lett. **8**, 2171 (2008).
[13] B. Kanté, A. de Lustrac, and J.-M. Lourtioz, Photonics Nanostruct. Fundam. Appl. **8**, 112 (2010).
[14] N. Liu, H. Liu, S. Zhu, and H. Giessen, Nat. Photonics **3**, 157 (2009).
[15] V. A. Fedotov, M. Rose, S. L. Prosvirnin, N. Papasimakis, and N. I. Zheludev, Phys. Rev. Lett. **99**, 147401 (2007).
[16] A. Ourir, R. Abdeddaim, and J. de Rosny, PIER **101**, 115 (2010).
[17] T. Q. Li, H. Liu, T. Li, S. M. Wang, F. M. Wang, R. X. Wu, P. Chen, S. N. Zhu, and X. Zhang, Appl. Phys. Lett. **92**, 131111 (2008).